Influence of the ethanol/dichloromethane ratio on the preparation of microsponges composed of ethylcellulose and Eudragit or HPMCphthalate for hydrophilic drug delivery

Mariana Volpato Junqueira, Sabrina Célia Calçado, Lidiane Vizioli de Castro-Hoshino, Mauro Luciano Baesso, Anna Szarpak-Jankowska, Rachel Auzély-Velty, Marcos Luciano Bruschi

Influence of the ethanol/dichloromethane ratio on the preparation of microsponges composed of ethylcellulose and Eudragit or HPMCphthalate for hydrophilic drug delivery

Mariana Volpato Junqueira[a,b], Sabrina Célia Calçado[b], Lidiane Vizioli de Castro[c], Mauro Luciano Baesso[c], Anna Szarpak-Jankowsa[d], Rachel Auzely-Velty[d], Marcos Luciano Bruschi[a,b]

[a]*Postgraduate Program in Pharmaceutical Sciences,* [b]*Laboratory of Research and Development of Drug Delivery Systems, Department of Pharmacy, State University of Maringa, 87020-900, Maringa, Parana, Brazil.*

[c]*Department of Physics, State University of Maringa, 87020-900, Maringa, Parana, Brazil.*

[d]*Centre de Recherches sur les Macromolécules Végétales, Université Grenoble Alpes, Grenoble, France.*

*****Corresponding author:

Tel: +55 44 3011 4870.

E-mail address: mlbruschi@uem.br (M. L. Bruschi).

ABSTRACT

Microsponges (MS) have shown great potential for the incorporation of relatively higher amounts of drugs. This is due to the presence of both surface pores and interconnected channels that provide a greater contact area for the absorption of active agents. However, the use of MS for carrying hydrophobic drugs is limited because the preparation methodology can totally remove hydrophilic drugs. Therefore, this work aimed to investigate possible changes in the proportion of organic solvents used to produce MS containing water-soluble drugs. A modified *quasi*-emulsion solvent diffusion technique was used to formulate MS with ethylcellulose and Eudragit RS 100 (MS-EE) or ethylcellulose and HPMCphthalate (MS-EH) using different combinations of ethanol/dichloromethane ratios. The effects of the polymeric composition and organic solvent ratio were evaluated on the morphology, size, swelling, yield, drug content, entrapment efficiency and *in vitro* release of methylene blue (MB), a hydrophilic drug model. Both polymer combinations resulted in spherical and porous particles. MS-EE was larger (8 – 13 μm) and displayed higher product yield (62 – 77%), but MS-EH showed a higher drug entrapment (11 – 41%), which was higher with an increase in the amount of ethanol amount used. Only MS-EH displayed *in vitro* MB release during 24 h (70%). ATR-FTIR and FT-Raman analyses did not demonstrate chemical interactions between MB and the polymers. Differential scanning calorimetry, thermogravimetry, and x-ray diffraction confirmed the molecular dispersion of MB in the MS polymer matrix. *Ex vivo* permeation studies by Franz cells and photoacoustic spectroscopy showed that MB could diffuse out from the polymer matrix and permeate both pig skin and mucosa. The particles were shown to be good carriers for MB and they provided controlled drug release and permeation through skin and mucous tissue; however, the MS particles themselves are not able to permeate these membranes. The use of ethanol in the solvent system constitutes a

good strategy to obtain MS of ethylcellulose and HPMCphthalate for delivery of MB and suggests that MS is worthy of investigation as carrier for delivery other hydrophilic drugs.

Keywords: ethylcellulose; Eudragit RS100; 2-hydroxypropyl methylcellulose phthalate; methylene blue; microsponges; drug delivery.

1. Introduction

Microparticles that are composed of a wide variety of polymeric materials (i.e., cellulose derivatives, other polysaccharides, or gelatine) can provide controlled drug release. Moreover, polymeric microparticles can be incorporated into oral or topical pharmaceutical dosage forms [1]. Microparticles can be classified into microcapsules (reservoir system) or microspheres (solid matrix systems). In microspheres, the polymeric material forms a three-dimensional network where the drug can be incorporated, absorbed or covalently bound to its surface. Besides that, the system may be homogeneous or heterogeneous depending on whether the drug is dissolved (molecular state) or suspended (particle form) [1, 2]. As a result of the process used, porous systems may be obtained; which these can also be referred to as microsponges (MS).

MS are a type of microspheres utilized as a drug delivery system. They display a rigid or malleable matrix that range in size from 5 to 300 μm, depending on their composition. They also can incorporate relatively high amounts of drugs into their numerous interconnected channels, which also aids in the maintenance of the spherical structure [2,3]. Another typical characteristic of MS is the presence of pores on the surface, which can control the drug release. A single 25-μm particle contains about 250,000 pores, which, together with the interconnected channels, gives an internal area of about three meters in length and a total volume of 1 ml/g of particle [4].

MS can be prepared by two distinct methodologies, liquid-liquid suspension polymerization or *quasi*-emulsion solvent diffusion [5,6]. The first method is utilized when the drug is capable of withstanding the conditions used during the polymerization and generation of the porous structure [6]. The second one is most often applied due to its simplicity and reproducibility. This methodology requires less organic solvent compared to the first one [7]. *Quasi*-emulsion methodology requires two phases (organic and the aqueous

phases). The aqueous phase is composed of a polyvinyl alcohol (PVA) dispersion [8]. Meanwhile, the organic phase contains polymers, especially ethylcellulose (EC) and Eudragit, the organic solvent (i.e. dichloromethane, ethanol and/or methanol) and the drug [2,3,7–27].

However, for *quasi*-emulsion methodology, the drug should be water-immiscible or only slightly soluble. Otherwise, it would not be possible to trap hydrophilic drugs in MS, because the step of forming the droplets would cause the drug to exit into the aqueous medium [28–30].

Therefore, this work investigated whether a modification of the solvent system of polymers [EC and Eudragit RS100 (ERS100) *versus* EC and 2-hydroxypropyl methylcellulose phthalate (HPMCph)] could improve the entrapment efficiency of hydrophilic drugs. These polymers are biologically inert, non-mutagenic, non-allergenic, non-toxic, non-irritating and non-biodegradable [31,32]. Besides that, HPMCph is a polyanionic molecule that possibly reacts with the positively charged group of methylene blue, preventing drug diffusion. Moreover, to decrease the amount of dichloromethane used for the MS preparation, different organic solvent proportions using a mixture with ethanol were tested.

2. Materials and methods

2.1. Materials

Methylene blue (MB) was purchased from Sigma-Aldrich (St. Louis, MO). Standard premium ethylcellulose (EC) NF 20 was supplied by Dow (São Paulo, Brazil), Eudragit RS100 (ERS100) was purchased from Evonik Pharma (Mumbai, India) and the 2-hydroxypropyl methylcellulose phthalate (HPMC phthalate; HPMCph) from Shin-Etsu Chemical (Tokyo, Japan). Polysorbate 80 was purchased from Synth (São Paulo, Brazil). Polyvinyl alcohol (PVA) and poloxamer 188 (P188) were purchased from Neon (Suzano, Brazil) and from BASF (Ludwisghaften, Germany), respectively. All other chemicals were

purchased from Nuclear (Diadema, Brazil) or Anidrol (Diadema, Brazil) and they were of analytical grade.

2.2. Preparation of microsponges

MS were prepared by the *quasi*-emulsion technique [33]. The polymeric solution (organic phase) was prepared using EC and ERS100 or EC and HPMCph in different ratios of ethanol:dichloromethane (Table 1). The porogenic solution was dropped in the organic phase to form a w/o emulsion. The porogenic solution was previously prepared with a 1% (v/v) aqueous solution of sodium chloride and a sufficient amount of polysorbate 80 to obtain 1% (v/v) dispersion; the MB (a drug model) is added at the end of this process with magnetic stirring. The w/o emulsion was dropped into an aqueous dispersion of PVA or P188. The resulting w/o/w emulsion remained under magnetic stirring during 24 h for organic solvent evaporation. The particles were separated by centrifugation at 15,000 rpm for 10 min; then the precipitate was dried at 40 °C in a hot air oven and stored in a desiccator until further analysis [34].

Table 1

Polymeric composition and organic solvent system utilized for the preparation of microsponges (MS).

Formulation	MB (%, w/w)	Porogenic solution (ml)	Organic phase			
			EC (%, w/w)	ERS100 (%, w/w)	HPMCph (%, w/w)	Ethanol:Dichrat
MS-EE-50	0.25	5.0	0.5	0.1	-	50:
MS-EE-70	0.25	5.0	0.5	0.1	-	30:
MS-EE-80	0.25	5.0	0.5	0.1	-	20:
MS-EE-100	0.25	5.0	0.5	0.1	-	0:1
MS-EH-50	0.25	5.0	0.5	-	0.03	50:
MS-EH-70	0.25	5.0	0.5	-	0.03	30:
MS-EH-80	0.25	5.0	0.5	-	0.03	20:
MS-EH-100	0.25	5.0	0.5	-	0.03	0:1

MB = methylene blue; EC = ethylcellulose; ERS100 = Eudragit RS100®; HPMCph = 2-hydroxypropyl methylcellulose phthalate; PVA = polyvinyl alcohol; P188 = poloxamer 188.

119

120

121 *2.3. Morphological analysis*

122 The surface morphology of MS was investigated by two different methodologies. For
123 the first analysis, the samples were coated with gold under argon atmosphere and observed in
124 a scanning electron microscope (Quanta) under two magnifications (x500 or x1000). The
125 second analysis was carried out using a fluorescence microscope (Axio observer 7, Carl Zeiss,
126 Germany) with software Zenblue. The fluorescence was evaluated with DAPI and/or GFP
127 filters with 25% of light source and 70 to 6000 µs of exposure time. For these analyses, the
128 MS samples were dispersed in water (1%, w/v).

129

130 *2.4. Particle size analysis*

131 The particle size analysis was carried out using dynamic light scattering analyser
132 (Nanoplus-3, Particulate Systems, USA). A 1% aqueous dispersion (w/v) of MS was used to
133 record the average particle diameter, polydispersity index, and zeta potential.

134

135 *2.5. Solubility properties of polymeric systems*

136 The solubility properties experiments were performed using an inverted microscope
137 (Axio observer 7, Carl Zeiss, Germany). The dry powder of MS (MS-EE-80 or MS-EH-80)
138 was placed into a Petri dish (32 mm) and 1.5 mL of ultrapure water or a 20% (v/v) ethanol
139 aqueous solution was added. Just after the contact of samples with water a picture was
140 captured (time 0) and another was taken of the same particles after standing overnight. The
141 diameter of 50 particles was determined by software ZenBlue (Carl Zeiss, Germany). The
142 solubility was assessed by the analysing the difference between the diameter at time 0 and
143 after 12 h.

144

145 *2.6. Determination of yield, drug content and entrapment efficiency*

146 The product yield was determined by dividing the practical weight of MS into the total
147 amount of drug and polymers used in the preparation of these particles times 100. To evaluate
148 the drug content and entrapment efficiency, 10 mg of MS were added in a 5 ml volumetric
149 flask containing 200 µl of methanol to disrupt the microparticles and extract the MB. After 10
150 minutes under ultrasound, the dispersion was filtered, and the absorbance was measured using
151 a UV-VIS double beam spectrophotometer (UV 18000 PC, Shimadzu, Tokyo, Japan) at a
152 wavelength of 664 nm. For the blank solution, the sample was composed of blank-MS. The
153 data were analysed by using a calibration curve obtained from a spectrophotometric method
154 that was previously developed and validated [35]. The drug content and the entrapment
155 efficiency were calculated according to equations below (1,2) [22,34,36]:

156

157 $$Drug\ content\ (\%) = (practical\ drug\ content\ in\ microsponges / theoretical\ weight\ of\ microsponges) \times 100 \quad (1)$$

158

$$Entrapment\ efficiency\ (\%) = (practical\ drug\ content\ in\ microsponges / theoretical\ drug\ content) \times 100 \quad (2)$$

2.7. Attenuated total reflectance-Fourier transform infrared spectroscopy (ATR-FTIR) and FT-Raman spectroscopy

The ATR-FTIR was performed for pure substances, their physical mixtures, and blank-MS and MS-MB using a Bruker FTIR spectrometer (VERTEX 70v, Ettlingen, Germany). The scanning range was from 400 to 4000 cm^{-1} with 250 scans and resolutions set at 4 cm^{-1}. FT-Raman spectra from the samples were recorded using the Bruker FT-Raman spectrometer (RAM II, Ettlingen, Germany) with radiation of 1064 nm from an Nd: YAG laser at 100 mW of power and liquid nitrogen cooled Ge detector. Each spectrum (range of 400 to 4000 cm^{-1} with 4 cm^{-1} of resolution) is the average of 250 scans [37].

2.8. Thermal analysis

Differential scanning calorimetry (DSC) and thermogravimetry (TGA) analysis (Q20 and Q50, T.A. Instruments, New Castle, USA) were performed in a compressed air atmosphere with a heating rate of 10 °C/min over a temperature range of 30 to 600 °C (TGA) and 30 to 200 °C (DSC). The samples (pure substances, their physical mixtures, blank-MS and MS-MB) were accurately weighed into aluminium pans and sealed.

2.9. X-ray analysis

X-ray diffraction analysis of polymers, drug, and MS were performed using an x-ray diffractometer D8 Advance, Bruker (Karlsruche, Germany) employing Cu-Kα radiation of wavelength 1.5405 Å, voltage 30 kV, and current 30 mA. The scans were run from 5 to 50º (2°/minute) 2θ [20].

184 *2.10. Evaluation of in-vitro drug release profile*

185 *In-vitro* MB release was assessed using a modified Franz's cell apparatus [37].
186 Purified water (20 ml) at 37 °C was utilized as a dissolution medium under constant magnetic
187 stirring (60 rpm). The amount of 30 mg of sample was placed directly into the release
188 medium, ensuring the sink conditions. At predetermined time intervals (30 min and 1, 2, 3, 4,
189 6, 8, 12 and 24 h), aliquots (2.0 ml) of the dissolution medium were withdrawn with
190 replacement of the same volume using release medium. The MB concentration was
191 determined by spectrophotometry (λ = 664 nm) according to the methodology previously
192 developed and validated [35]. To investigate the mechanism of MB release from MS, the data
193 generated from these release studies were fitted to the general equation (Equation 3) using
194 logarithmic transformations and least-squares regression analysis [38].

195

196 $$Mt/M\infty = k.t^n \quad (3)$$

197

198 Where $Mt/M\infty$ is the fraction of released drug, t is the time of release, k is the kinetic constant
199 of incorporation of the structural and geometric characteristics of the release device, and n is
200 the exponent that might indicate the mechanism of drug release.

201

202 *2.11. Ex-vivo study of MB permeation from MS*

203 *2.11.1. Preparation of biological tissues*

204 Ear skin and buccal mucous samples were obtained from white, young, and recently
205 slaughtered pigs (from a slaughterhouse authorized for human consumption by the Brazilian
206 Ministry of Agriculture). Skin tissues were cleaned with purified water, the subcutaneous fat
207 was gently removed and a skin square sample from the central region of the dorsal side of the
208 auricle was excised using scissors and a surgery scalpel. Buccal mucosa tissues were also

cleaned with purified water and the mucous layer was carefully separated from the muscle and adipose tissue. Samples with wounds, warts, or hematomas were not used.

2.11.2. Permeation study using Franz cells apparatus

Tissue samples (skin or mucosa) were placed between the donor and receptor chambers of the cell with the dermal side or mucous layer in contact with the receptor medium. The receptor chamber was filled with phosphate buffer (pH 7.4) and kept at 37.0 ± 1 °C. The amount of 20 mg of MS-EH-MB was applied to the tissue. Samples of 0.50 ml were withdrawn from the receptor medium (with a replacement of the same volume) at 30 min and 1, 2, 3, 4, 6, 8 and 24 h. Sink conditions were maintained in all cases, and the absence of air bubbles was checked after each replacement. The MB concentration was analysed by spectrophotometry (λ = 664 nm), according to methodology previously developed and validated [35] and determined on the basis of the available area for permeation; these values were plotted as a function of time ($\mu g.cm^{-2}.min^{-1}$) [39,40].

2.11.3. Retention study

MB cutaneous retention was performed after the end of the skin permeation study. *Stratum corneum* (SC) was then tape-stripped 40 times, using an adhesive tape (Scotch 3M). Permeation area of the epidermis (without SC) + dermis was then separated with scissors. The MB contents in tape stripes and also in epidermis (without SC) + dermis were extracted using methanol. The extractive solutions were analysed by spectrophotometry (λ = 664 nm) and the amount of MB was calculated according to Equation (4) [41].

$$Q_{real} = \left(C_{measured,t}/D\right)V + \sum Q_{real,t^{-1}} \quad (4)$$

Where Q_{real} is the accumulated permeated amount, $C_{measured,t}$ is the concentration measured from the sample at time t, D is the dilution factor, V is the volume of Franz's cell, and $Q_{real,t}^{-1}$ is the accumulated permeated amount at time t^{-1}. The value of MB permeated was plotted as a function of time ($\mu g.cm^{-2}$) [40].

For determination of MB retention or permeation in mucosal tissue, the methodology for drug extraction from mucosa and analytical methodology were the same.

2.11.4. Determination of skin and mucous permeation by photoacoustic spectroscopy (PAS)

The measurements were performed on sections of skin and mucous from pigs (1 cm^2), 30 minutes after applying 50 µl of aqueous dispersion (3.5%, w/v) of MS-blank (negative control) or MS-MB. The PAS experimental setup was composed of an 800 W Xenon arc lamp that was used as the light source. The light was diffracted by passing through the monochromator with 3.16-mm input and output slots. The monochromator was equipped with a diffraction grade for the UV–Vis spectral range from 200 to 800 nm. The mechanical chopper was tuned at 13 Hz modulating the light that impinges the sample. Thus, the monochromatic beam was focused on the sample placed inside the photoacoustic cell, which was sealed with a transparent quartz window (8 mm diameter and 2 mm thickness). A capacitive microphone was coupled to collect the photoacoustic signal that was generated from the pressure variation resulting from the periodic heating of the sample. The depth of the skin sample contributing to the photoacoustic signal was estimated using the thermal diffusion length of 31 µs. The final photoacoustic signal is proportional to the sample absorption coefficient, and then the photoacoustic spectra can be interpreted through absorption bands. In all analyses, the skin was evaluated on apical (epidermis) and basal (dermis) layers [42–44].

3. Results and discussion

3.1. Morphology and particle size

The particles prepared from EC:ERS100 or EC:HPMCph mixtures with an equal proportion of ethanol and dichloromethane displayed the largest amorphous structures (Figure 1).

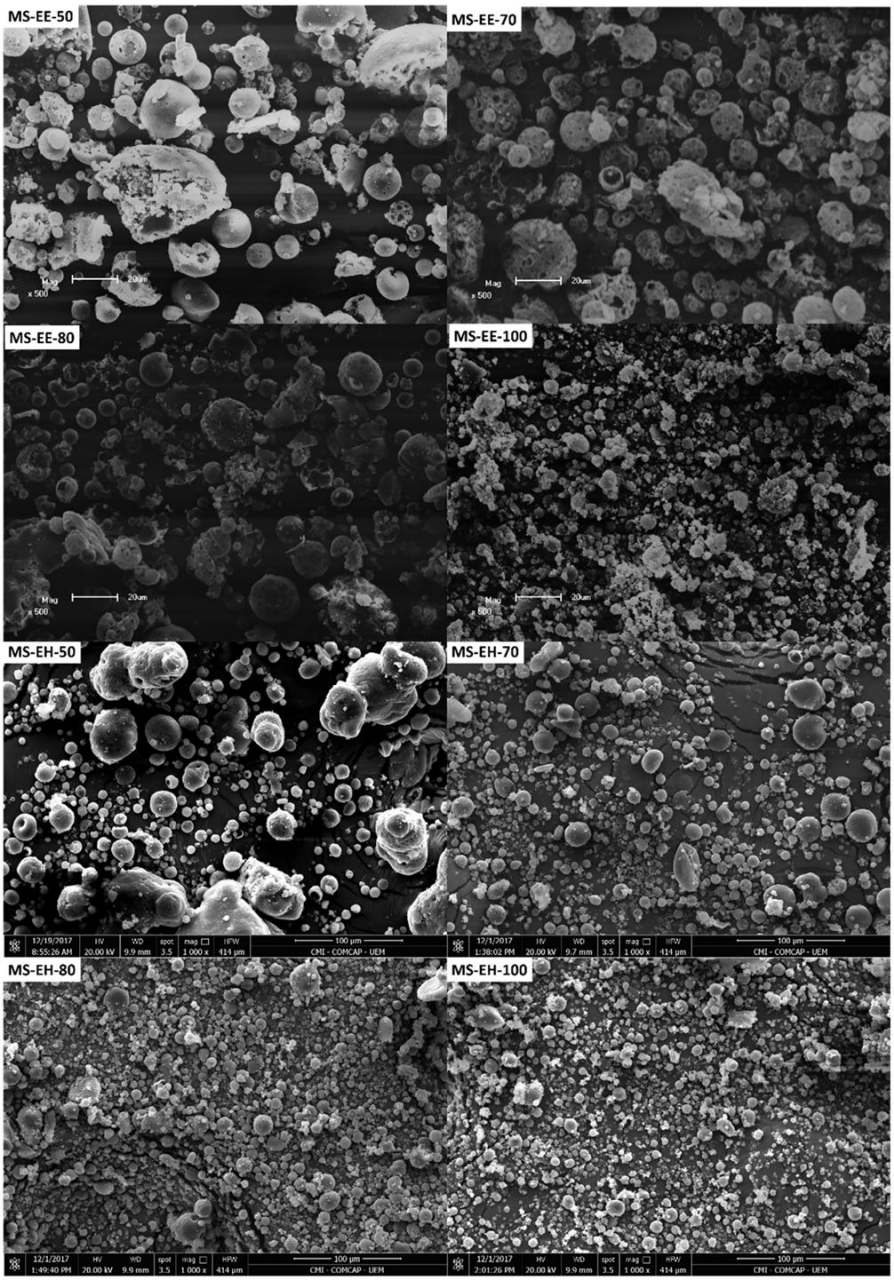

Fig. 1. SEM images of MS-EE and MS-EH prepared using 0, 20, 30 or 50% (v/v) of ethanol (original magnification: x500 (MS-EE); x1000 (MS-EH)).

Decreasing the ethanol proportion promoted the formation of small and homogenous particles, which can be confirmed by size analysis (Table 2). It is known that the size of the particles is influenced by several factors. Among these are the volume and ratio of organic solvents. In this sense, those that exhibit higher vapor pressure lead to an increase in kinetic energy which consequently increases the diffusion of solvent from the organic solution to air, producing smaller particles [3,32]. Another factor that can influence the size is the drug: polymer ratio [45]. Particulate systems produced with higher polymer concentration are larger due to the higher availability of these substances; this occurred with MS-EE which present about 10% more polymers than MS-EH.

Table 2

Evaluation data of methylene blue (MB) loaded microsponges prepared with ethylcellulose-Eudragit RS100 (MS-EE) or ethylcellulose:HPMCph (MS-EH) in different organic solvent ratios (ethanol:dichloromethane, 50:50; 40:60; 30:70; 0:100).

Formulation	Particle size (μm)	PDI*	Product yield (%, w/w)	MBcontent (%, w/w)	Entrapment efficiency (%, w/w)
MS-EE-50	12.92	4.06	62.30 ± 29.66	0.003 ± 0.000	1.29 ± 0.01
MS-EE-70	11.34	2.86	69.12 ± 15.42	0.003 ± 0.000	1.47 ± 0.03
MS-EE-80	9.05	5.07	70.56 ± 19.68	0.003 ± 0.000	1.50 ± 0.01
MS-EE-100	7.91	0.46	77.38 ± 12.54	0.003 ± 0.000	1.25 ± 0.00
MS-EH-50	7.44	1.59	52.79 ± 1.41	0.103 ± 0.000	41.35 ± 0.15
MS-EH-70	4.47	0.37	49.59 ± 0.92	0.062 ± 0.001	25.12 ± 0.26
MS-EH-80	3.48	0.26	48.21 ± 0.97	0.045 ± 0.000	18.01 ± 0.55
MS-EH-100	2.26	0.70	44.82 ± 0.67	0.027 ± 0.001	10.78 ± 0.20

*PDI = polydispersity index

279 Moreover, MS composed of EC-ERS100 and EC- HPMCph possess a porous surface,
280 independent of the organic solvent concentration used (Figure 2). These results showed that
281 both combinations of polymers could produce spheres with characteristics of MS.
282

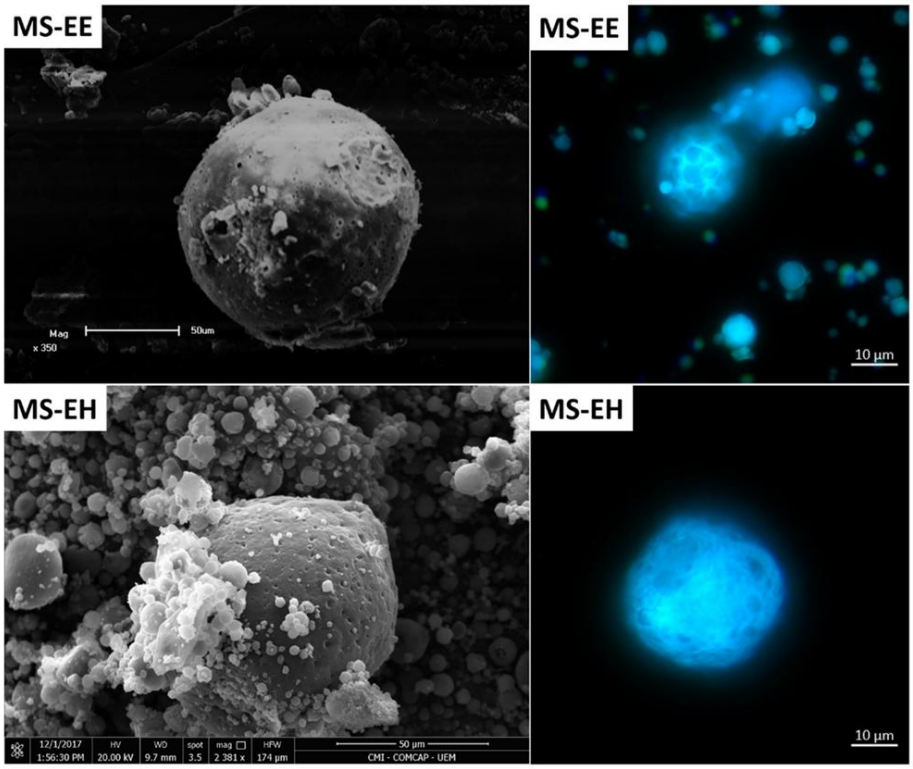

283

284 **Fig. 2.** SEM and fluorescence images of porous on the surface of MS-EE and MS-EH
285 microsponges (SEM original magnification x350 (MS-EE), x2381 (MS-EH); fluorescence for
286 both MS is original magnification x400).
287

288 *3.2. Solubility properties of systems*

289 The solubility of MS was evaluated by monitoring the increase of particle diameter
290 after a predetermined time interval. The diameter can be changed due to the solvent
291 penetration into the particles and, consequently, the solubility properties of polymers used for
292 the preparation. Figure 3 displays the effect of ultrapure water and ethanol solution on MS.
293 No solubility process was observed after 12 h in both cases. It is known that Eudragit RS 100

shows water solubility [46]. Moreover, a low solubility rate was already expected in MS-EH since HPMCph presents this property. However, as the concentrations of these two polymers are 17 times lower than EC, their presence did not display a significant influence on the parameter ($p > 0.05$).

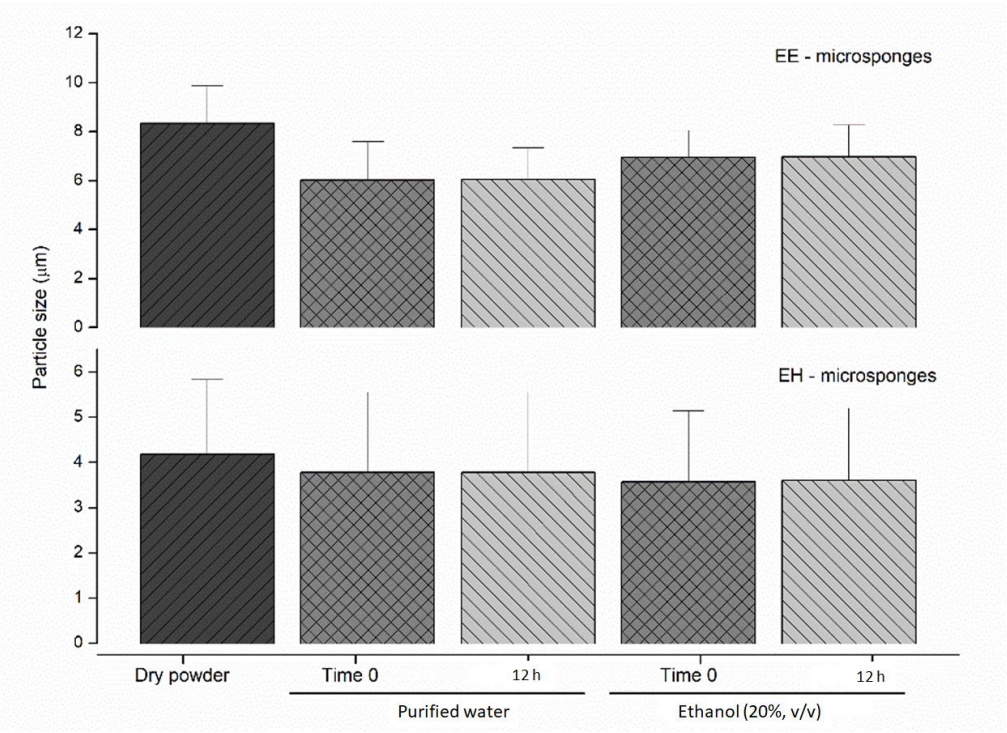

Fig. 3. Results of solubility analysis of methylene blue loaded microsponges at the time 0 and after 12 h in purify water or ethanol solution 20% (v/v).

3.3. Product yield, drug content and entrapment efficiency

The yield of MS-EE was about 43% higher than those prepared with HPMCph (Table 2). This difference can be explained by the change of polymer used with EC. Studies that used the EC-Eudragit combination showed equal or even higher yields than those observed in MS-EE, demonstrating that even small changes in the preparation methodology may influence this parameter's results [7,16,18,32]. The use of different compositions of organic solvent was

309 only relevant for the MS-EH, where the lower the volume of dichloromethane, the higher the
310 yield.

311 The volume and different types of solvent used also influenced the drug content and
312 entrapment efficiency. Organic solvents that have a lower evaporation rate have lower kinetic
313 energy; consequently, this reduces the diffusion rate of the solvent from the internal to the
314 external phase and increases the probability of entrapping the hydrophilic drug within the MS
315 [32]. Thus, MS prepared with higher volumes of ethanol have higher entrapment efficiencies.
316 However, high polymer concentrations provide larger particles, which require more time to
317 become rigid, and this increases the time available for drug diffusion out of the MS [8], as can
318 be observed for MS-EE.

319

320 *3.4. In-vitro drug release profile*

321 The MS physicochemical characteristics were investigated in order to understand the
322 behaviour of system aiming the future development of drug delivery systems to be
323 administered locally (e.g. skin and mucosae). Therefore, topical administration would suggest
324 a temperature of 32 °C. However, this temperature can be higher when the administration is in
325 the mucosa of different regions of the organism such as vaginal, buccal, nasal, and rectal
326 [41,43]. In this sense, the analyses were performed considering the temperature of 37 ºC.
327 Moreover, the MS are proposed for local administration, and since MB is highly soluble in
328 water, the release test was performed using an aqueous medium as the first step to understand
329 the system behaviour. Biorelevant media should be used in the future. An inert membrane
330 (e.g. cellulose acetate membrane) is frequently used for the *in vitro* drug release tests using
331 Franz cells, modified Franz cells, or other apparatus as a support to separate the donor
332 compartment from the acceptor compartment [37]. Sometimes the presence of this membrane
333 influences the drug release constituting a limiting aspect. In this study, we have firstly

334 performed a test with cellulose a acetate membrane, but the drug could not be released
335 properly [41,43]. Thus, considering the size of particles, the formulation was placed inside the
336 acceptor compartment together with the release medium. Therefore, the test setup was
337 prepared without membrane support and it was possible to withdraw the samples at the pre-
338 determined time intervals without removing particles from the dissolution medium.

339 The *in-vitro* MB release profile was not performed with MS-EE-MB despite the fact
340 this sample presented a low entrapment efficiency and drug content. The results found are
341 below the detection and quantification limits for the methodology used for the quantification.
342 As indicated in the mentioned tests, this system does not prove to be a viable alternative for
343 the entrapment of hydrophilic drug. This may be associated with the process chosen to
344 prepare the MS. There was diffusion of the MB to the external phase due to the greater
345 affinity for the aqueous medium.

346 Therefore, it would be expected that the same would happen for the MS-EH-MB
347 system. However, the MB release from this system reached almost 70% in 24 h (Figure 4).
348 Also, the drug release occurred gradually, which was also not expected for a hydrophilic drug.
349 This unexpected result can be explained by the use of HPMCph, because it is a polyanionic
350 polymer that possibly interacted with positively charged group of MB. This would prevent the
351 drug from diffusing into the aqueous phase during the preparation. Moreover, this system
352 could provide an MB modified release in relationship to pure MB (Figure 4). The inherent
353 dissolution of pure MB in water does not represent the release, but it was performed as a
354 comparative (as a reference) considering the influence of the protocol utilized to determine
355 the MB release profile from microsponges.

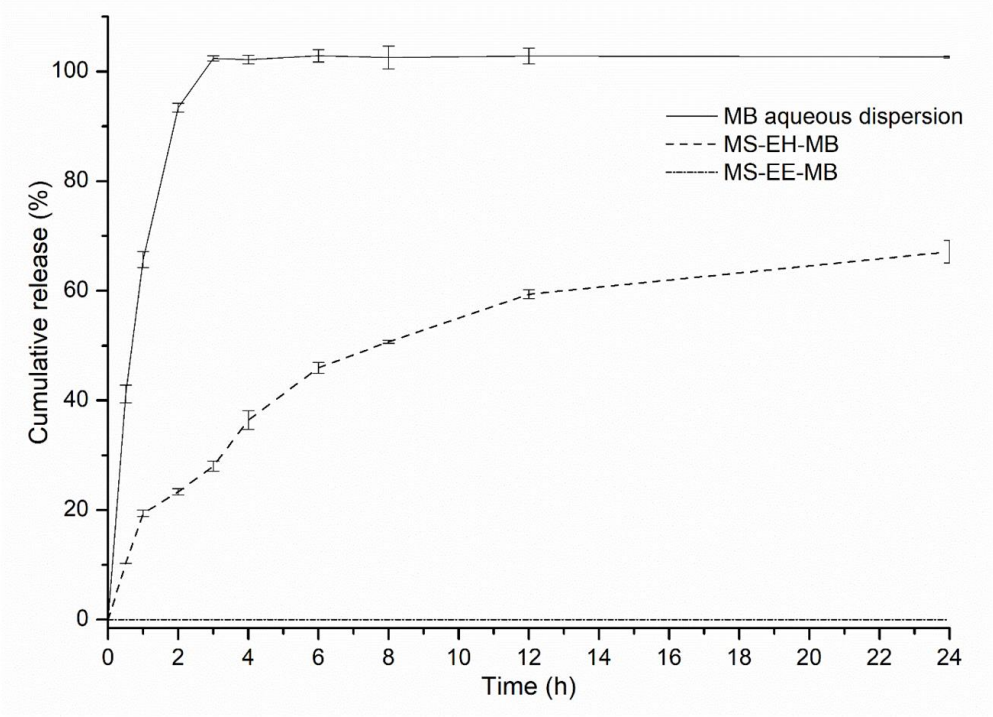

Fig. 4. *In-vitro* release profile of methylene blue (MB) from aqueous dispersion (0.25%, w/w) and from microsponges MS-EE-MB and MS-EH-MB.

As mentioned before, the MB from MS-EH-MB showed prolonged release; therefore, it was a better fit with the Korsmeyer-Peppas equation. Besides, the kinetic release parameters were calculated in order to evaluate the mechanism involved in the release of MB. For spherical structures, an n-value = 0.43 indicates controlled release by Fickian diffusion, and n = 0.85 indicates that release occurs by relaxation of polymer chains (transport Case II). Values within this range indicate anomalous behaviour, i.e., the diffusion process and polymeric chains swelling influence the release. The observed n-value (0.523) indicates that MB release was governed by diffusion through the MS channels and by HPMCph swelling (anomalous behaviour) [9,47]. The discrepancy with the swelling test could be related to the low degree of swelling and a low concentration of the HPMCph, which was shown to be incapable of changing the particle size but could influence the drug release.

372 *3.5. Drug–polymer interaction study for MS-EH*

373 To evaluated the physical states and the stability of materials and to ensure the drug-
374 polymer compatibility and interaction, ATR-FTIR, FT-Raman, TGA, DSC and X-ray powder
375 diffraction analyses were performed [34,48]. These analyses were used for evaluating MS
376 prepared with EC and HPMCph, because they gave the best results for drug content,
377 entrapment efficiency, and *in-vitro* drug release.

378 The ATR-FTIR spectra of EC (Figure 5a), HPMCph (Figure 5b), MB (Figure 5c),
379 blank-MS-EH (Figure 5d), and MS-EH-MB (Figure 5e) are shown in Figure 5. Spectra of MB
380 showed bands at 3371 cm^{-1} (N-H stretching of aliphatic primary amine), 1595 cm^{-1} (N-H
381 bending of secondary amine), 1488 and 1332 cm^{-1} (aromatic nitro compounds), 1390 cm^{-1}
382 (deformation of multiplet C-H), 1139 cm^{-1} (N-H of tertiary amine), and 879 cm^{-1} (aromatic C-
383 H). However, for blank-MS and MS-MB, their spectral analysis appeared with prominent
384 peaks characteristics of EC (3485, 2976-2869, 1375, and 1035 cm^{-1}), one peak of HPMCph
385 (1726 cm-1), and in both cases MB peaks are absent. These results suggest no chemical
386 interaction or changes during the preparation process and MB stabilization into MS. The
387 Raman spectrum of MB showed bands with two peaks, one at 1625 and other at 1400 cm^{-1}
388 (C-C ring stretching and C-N symmetrical stretching, respectively). In contrast to the ATR-
389 FTIR spectra, it is possible to observe both characteristic peaks of a pure drug in the FT-
390 Raman spectra for MS-MB.

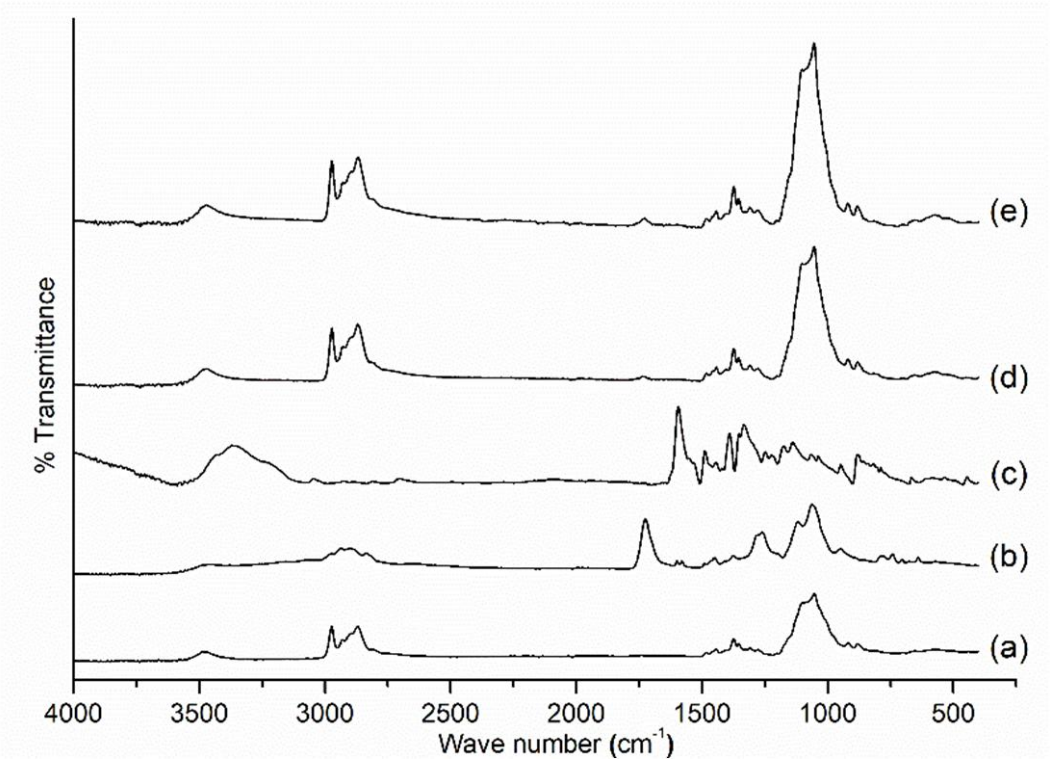

Fig. 5. ATR-FTIR spectra of: (a) ethylcellulose, (b) HPMCph, (c) methylene blue, (d) MS-EH-blank and (e) MS-EH-MB.

Figure 6.1c shows the thermogram and first derivative thermogram of the drug, where is possible to observe peaks for four steps. The first two steps correspond to the loss of hydration water (between 50 and 100 °C) with a weight loss of approximately 19%. The next step, between 170 and 190 °C, is related to decomposition reaction with a loss of around 23%. In the last one the pure drug mass reached 2% of the initial weight; that is, the MB is almost completely degraded as temperatures reach 340 and 540 °C. For EC (Figure 6.1a), the decomposition occurs in two steps (200 and 340 °C), where the weight loss was about 87%, and another, between 420 and 440 °C, where the weight percentage decreased to approximately 0% of the initial value. For HPMCph (Figure 6.1b), the decomposition was above 160 °C with a weight loss of 40%, then a more pronounced loss at 350 °C where the residual mass was only 9% of the original. The physical mixture (Figure 6.1d) and MS-EH-

MB (Figure 6.1e) showed curves more similar to those of EC, which is present in high amounts, but the decomposition occurs at a lower temperature, when compared to isolated polymer, especially in samples of MS. This indicates a possible interaction between the polymers components and the drug.

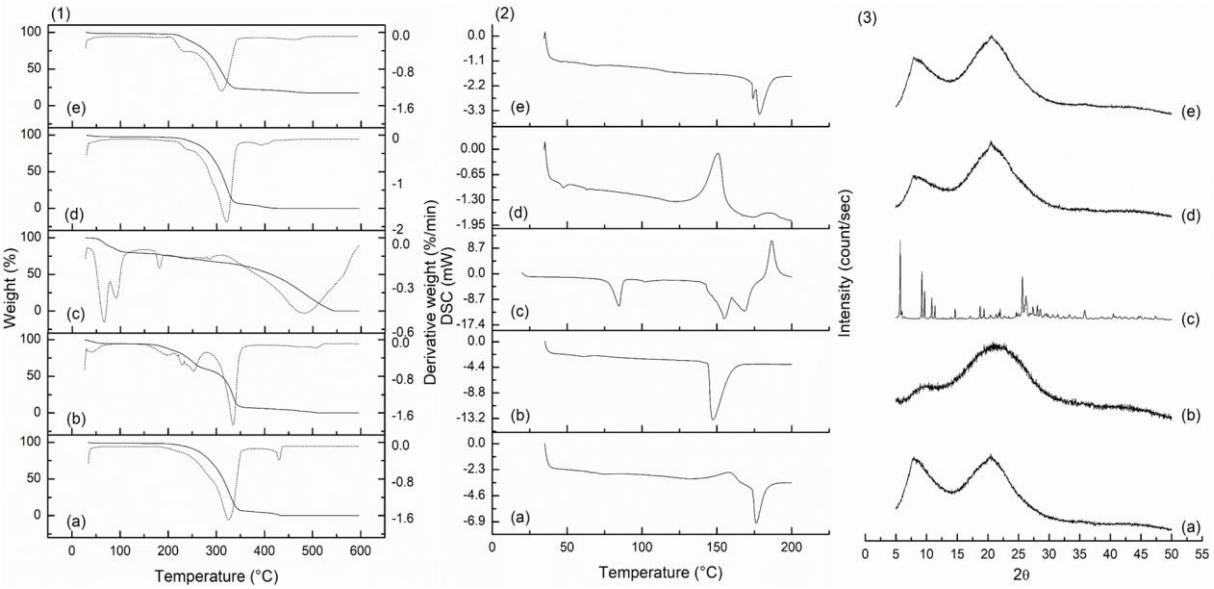

Fig. 6. (1) Thermogravimetric analysis (TGA, solid line) and derivative thermogravimetric (DTG, dash line) curves, (2) DSC thermograms, and (3) X-ray diffraction patterns of: (a) ethylcellulose, (b) HPMCph, (c) methylene blue, (d) MS-EH-blank and (e) MS-EH-MB.

The DSC curves of MB (Figure 6.2c) showed peaks in the region of 90 - 110 °C, corresponding to the melting point of the compound [49]. Moreover, more two endodermic peaks were displayed in the region of 154 - 167 °C, corresponding to the drug decomposition [49]. The thermogram of EC (Figure 6.2a) and HPMCph (Figure 6.2b) presents peaks at around 177 °C and 150 °C; these represent the softening transition, which depicts its semi-crystalline nature, and a glass transition depicting its amorphous state, respectively [34,50,51]. The thermogram of MS-EH-MB (Figure 6.2d) showed two endothermic peaks at around 170

°C, indicating as a possible interaction between the polymers with the MB as well partial protection of the drug by the structure of MS.

X-ray powder diffraction patterns of MB, EC, MS-EH-blank, and MS-EH-MB are displayed in Figure 6.3. Sharp peaks were observed for MB (Figure 6.3c) at diffraction angles of (2θ) 5.68°, 9.22°, 9.67°, 10.83°, 11.34°, 14.65°, 18.73°, 19.38°, 25.64°, and 26.23°, indicating a crystalline nature of the pure drug. Both samples of MS, blank (Figure 6.3d), and MB-loaded (Figure 6.3e) displayed a broad peak that is characteristic of an amorphous structure. The polymers EC (Figure 6.3a) and HPMCph (Figure 6.3b) also presented a broad peak without diffraction. These results could indicate that the crystalline nature of MB was completely lost, and there was not a recrystallization process during the evaporation and/or drying steps. This MS amorphous state indicates that the systems have a better condition to promote the MB release. Thus, the drug is probably totally dispersed in the polymeric matrix [37].

3.6. *Permeation studies*

During the development of new systems is important to understand the behaviour in different conditions. The results of this study can be utilized for the selection of the best formulation candidates for the future design of microsponges for the delivery of different hydrophilic drugs to be administered locally on skin and mucosae. The permeation of substances through the skin or mucous membranes is related to physicochemical proprieties when incorporated into complex systems. In the skin case, the permeation depends on the presence of natural barriers that block the entry of several components, such as *stratum corneum* (SC) [52]. Even knowing this, the study was conducted with full thickness skin to investigate the microparticulate system's influence on penetration and permeation of the skin

by MB released from the microsponges. For oral mucous, the drug permeation is associated with keratinization degree and thickness [53,54].

The permeation analyses performed using Franz cells apparatus shows that MB can diffuse out from the MS and completely permeate the oral mucous tissues only. It is known that mucous presents a permeation of around 4 and 4000 times greater when compared to the skin [53]. Another point to consider is the hydrophilic nature of MB, because the skin has a hydrophobic barrier that hinders the passage of substance with an affinity for water, as was already observed [41]. After 24 h, the amount of MB present in SC was determined, as well as in epidermis without SC + dermis and oral mucous tissues (Figure 7). The results support that skin acts to prevent the drug from passing through these layers (MB penetration, but not MB permeation). Despite MB being a hydrophilic substance, it could pass through the barrier *stratum corneum* and reach epidermis and dermis. The log P of MB (5.85) [55,56] should be considered, which would justify the relative affinity for the lipophilic regions of the skin. Microsponges acted as a finite MB reservoir, and after 24 h a drug concentration gradient was evident in skin, considering that the MB amounts in epidermis and dermis were determined together.

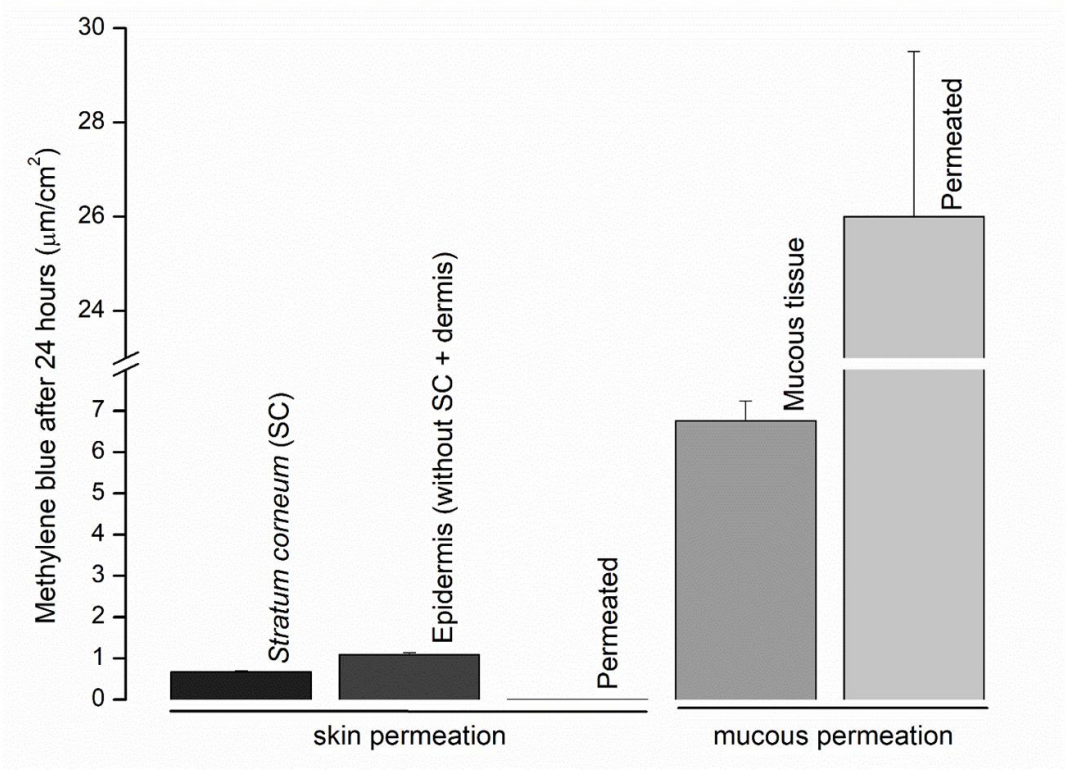

Fig. 7. Amount of methylene blue (MB) present in *stratum corneum* (SC), epidermis without SC + dermis, permeated through the skin after 24 h, and mucous permeation (mucous tissue retention and permeation).

In addition, the skin and mucous MS permeability was also investigated by PAS. This technique allows the analysis of low concentration, optically opaque and highly scattering samples in complex biological systems such as the skin and mucous tissues [43,57,58]. PAS can be employed to determine the absorption characteristics of the products topically applied and define the depth of penetration [58].

Figure 8a displays the photoacoustic spectra of MB and MS-EH-MB, where the presence of three peaks can be observed (300, 500, and 700 nm). The MS-EH-blank presented an absorption band between 200 and 450 nm. Figures 8b, 8c, and 8d present the spectra obtained from readings on the epidermis, dermis and mucous, respectively. In the mucous control spectra, it is possible to observe a band near to 400 nm, which is a characteristic of the

presence of blood. After 30 min in contact with the MB-aqueous solution, the biological tissues showed similar spectra when compared to a solution without the tissues. When in contact with the epidermis, dermis and mucous, the MS-EH-blank did not show the absorption band. That is, the MS demonstrated no ability to cross and permeated the layers due to its large size. However, as the MS-EH-MB was applied the tissues displayed absorbance between 550 and 700 nm, demonstrating that the drug was able to diffuse out from MS and cross all skin layers and oral mucous. In this sense these particles can be considered to be a good carrier for drugs.

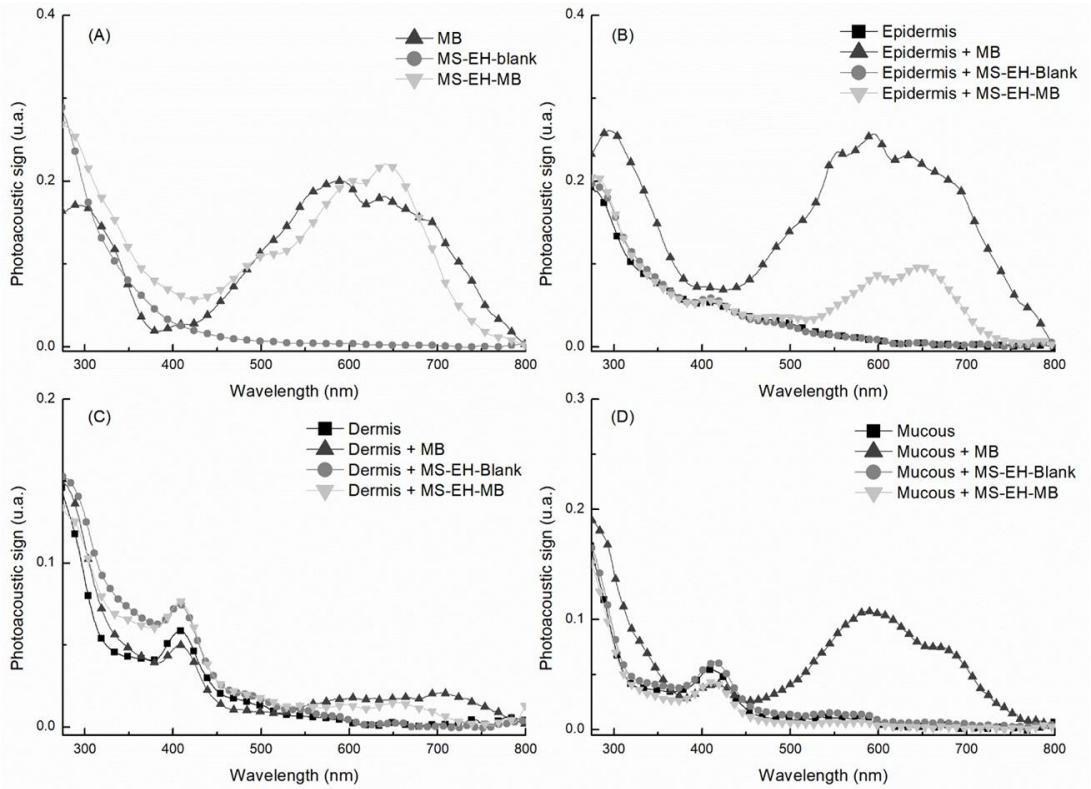

Figure 8.

4. Conclusions

Both polymer combinations could be used to prepare microsponges with spherical shape, porous surface, and interconnecting channels. However, only the microsponges

composed of ethylcellulose and HPMCphthalate could entrap methylene blue, the hydrophilic model drug. The presence of different ethanol proportions in the organic phase during the preparation of microsponges provided particles with different physicochemical characteristics. An increase of dichloromethane ratio provided particles with a smaller size, lower product yield, drug content, and entrapment efficiency when compared to microsponges prepared with the same volume of ethanol and dichloromethane. Moreover, the system composed of ethylcellulose and HPMCph showed a modified and constant drug release after 12 h. The particles were shown to be a good carrier for the methylene blue allowing controlled drug release and permeation through skin and mucous tissue; however, the microsponges are not able to permeate these membranes. Therefore, the utilization of ethanol in the solvent system constitutes a good strategy to obtain microsponges of ethylcellulose and HPMCph for delivery of methylene blue, and this suggests that this system is worthy of investigation as a carrier for delivery other hydrophilic drugs.

Acknowledgments

The authors are grateful to CAPES (*Coordenação de Aperfeiçoamento de Pessoal de Nível Superior*/Coordination for the Improvement of Higher Education of Brazil; grant number 88887.205259/2018-00), CAPES/COFECUB (grant number 917/2018) and CNPq (*Conselho Nacional de Desenvolvimento Científico e Tecnológico*/National Counsel of Technological and Scientific Development of Brazil), and FINEP (*Financiadora de Estudos e Projetos*/Financier of Studies and Projects of Brazil). The authors acknowledge the State University of Maringá (Brazil) and *Centre de Recherches sur les Macromolécules Végétales* (France) for supporting the project.

References

519 1. Mendes JBE. Desenvolvimento e avaliação de micropartículas poliméricas contendo
520 resveratrol. 2011.
521 2. Crcarevska MS, Dimitrovska A, Sibinovska N, Mladenovska K, Raicki RS, Dodov
522 MG. Implementation of quality by design principles in the development of
523 microsponges as drug delivery carriers: Identification and optimization of critical
524 factors using multivariate statistical analyses and design of experiments studies. *Int J*
525 *Pharm*. 2015;489(1-2):58-72. doi:10.1016/j.ijpharm.2015.04.038
526 3. Srivastava R, Pathak K. Microsponges: a futuristic approach for oral drug delivery.
527 *Expert Opin Drug Deliv*. 2012;9(7):863-878. doi:10.1517/17425247.2012.693072
528 4. Nokhodchi A, Jelvehgari M, Siahi MR, Mozafari MR. Factors affecting the
529 morphology of benzoyl peroxide microsponges. *Micron*. 2007;38(8):834-840.
530 doi:10.1016/j.micron.2007.06.012
531 5. Ravi R, Senthilkumar SK, Parthiban P. Microsponges drug delivery system: a review.
532 *Int J Pharm Rev Res*. 2013;3(1):6-11.
533 6. Patil RS, Kemkar VU, Patil SS. Microsponge Drug Delivery System : A Novel Dosage
534 Form. *Am J PharmTech Res*. 2012;2(July):227-251.
535 7. Annu P, Kumar AY. Design and Evaluation of CelecoxibMicrosponge. *Int J Pharma*
536 *Sci Res*. 2016;7(10):396-405.
537 8. Singh S, Pathak K. Assessing the bioadhesivity of Acconon MC 8-2 EP/NF for
538 gastroretention of floating microsponges of loratadine and achieving controlled drug
539 delivery. *Pharm Biomed Res*. 2016;2(2):58-74. doi:10.18869/acadpub.pbr.2.2.9
540 9. Muralidhar P, Bhargav E, Srinath B. Fomulation and optimization of bupropion HCl
541 microsponges by 23 factorial design. *Int J Pharm Sci Res*. 2017;8(3):1134-1144.
542 doi:10.13040/IJPSR.0975-8232.8(3).1134-44
543 10. Kumar PM, Ghosh A. Development and evaluation of metronidazole loaded

544 microsponge based gel for superficial surgical wound infections. *J Drug Deliv Sci*
545 *Technol*. 2015;30:15-29. doi:10.1016/j.jddst.2015.09.006
546 11. Amrutiya N, Bajaj A, Madan M. Development of Microsponges for Topical Delivery
547 of Mupirocin. *AAPS PharmSciTech*. 2009;10(2):402-409. doi:10.1208/s12249-009-
548 9220-7
549 12. Zhang C, Niu J, Chong Y, Huang Y, Chu Y, Xie S. Porous microspheres as promising
550 vehicles for the topical delivery of poorly soluble asiaticoside accelerate wound healing
551 and inhibit scar formation in vitro & in vivo. *Eur J Pharm Biopharm*. 2016;109:1-13.
552 doi:10.1016/j.ejpb.2016.09.005
553 13. Kumar JR, Muralidharan S, Ramasamy S. Microsponges enriched gel (MEGs): A
554 novel strategy for opthalmic drug delivery system containing ketotifen. *J Pharm Sci*
555 *Res*. 2013;5(4):97-102.
556 14. Li S, Li G, Liu L, et al. Evaluation of Paeonol Skin-Target Delivery from Its
557 Microsponge Formulation : In Vitro Skin Permeation and In Vivo Microdialysis. *PLoS*
558 *One*. 2013;8(11):1-8. doi:10.1371/journal.pone.0079881
559 15. Nokhodchi A, Jelvehgari M, Siahi MR, Mozafari MR. Factors affecting the
560 morphology of benzoyl peroxide microsponges. *Micron*. 2007;38:834-840.
561 doi:10.1016/j.micron.2007.06.012
562 16. Bhandare CR, Katti SA. Formulation of microsponges of risperidone HCl. *Int J Res*
563 *Pharm Chem*. 2016;6(3):518-527.
564 17. Çomoglu T, Gönül N, Baykara T. Preparation and in vitro evaluation of modified
565 release ketoprofen microsponges. *Farm*. 2003;58:101-106.
566 18. Mehta M, Panchal A, Shah VH, Upadhyay U. formulation and in-vitro evaluation of
567 controlled release microsponge gel for topical delivery of clotrimazole. *Int J Adv*
568 *Pharm*. 2012;2(2):93-101.

569 19. Kumar PM, Ghosh A. Development and evaluation of silver sulfadiazine loaded
570 microsponge based gel for partial thickness (second degree) burn wounds. *Eur J Pharm*
571 *Sci*. 2017;96:243-254. doi:10.1016/j.ejps.2016.09.038
572 20. Bothiraja C, Ghopal AD, Shaikh K, Pawar AP. investigation of ethyl cellulose
573 microsponge gel for topical delivery of eberconazole nitrate for fungal therapy. *Ther*
574 *Deliv*. 2014;5:781-794.
575 21. Orlu M, Cevher E, Araman A. Design and evaluation of colon specific drug delivery
576 system containing flurbiprofen microsponges. *Int J Pharm*. 2006;318:103-117.
577 doi:10.1016/j.ijpharm.2006.03.025
578 22. Osmani RAM, Aloorkar NH, Ingale DJ, et al. Microsponges based novel drug delivery
579 system for augmented arthritis therapy. *Saudi Pharm J*. 2015;23(5):562-572.
580 doi:10.1016/j.jsps.2015.02.020
581 23. Pande V V, Kadnor NA, Kadam RN, Upadhye SA. Fabrication and Characterization of
582 Sertaconazole Nitrate Microsponge as a Topical Drug Delivery System. *Indian J*
583 *Pharm Sci*. 2015;77(6):675-680. doi:10.4103/0250-474X.174986
584 24. Jain V, Jain D, Singh R. Factors Effecting the Morphology of Eudragit S-100 Based
585 Microsponges Bearing Dicyclomine for Colonic Delivery. *J Pharm Sci*.
586 2010;100(4):1545-1552. doi:10.1002/jps
587 25. Charagonda S, Puligilla RD, Ananthula MB, Bakshi V. Formulation and evaluation of
588 famotidine floating microsponges. *Int Res J Pharm*. 2016;7(4):62-67.
589 doi:10.7897/2230-8407.07440
590 26. Kadam V V., Patel VI, Karpe MS, Kadam VJ. Design, Development and Evaluation of
591 Celecoxib-Loaded Microsponge-Based Topical Gel Formulation. *Appl Clin Res Clin*
592 *trials Regul Aff*. 2016;4(3):44-55.
593 27. Jelvehgari M, Siahi-shadbad MR, Azarmi S, Martin GP, Nokhodchi A. The

microsponge delivery system of benzoyl peroxide : Preparation , characterization and release studies. *Int J Pharm*. 2006;308:124-132. doi:10.1016/j.ijpharm.2005.11.001

28. Kawashima Y, Niwa T, Takeuchi H, Hino T, Ito Y. Control of prolonged drug release and compression properties of ibuprofen microsponges with acrylic polymer, eudragit RS, by changing their intraparticle porosity. *Chem Pharm Bull*. 1992;40(1):196-201. doi:10.1248/cpb.40.196

29. Jain N, Sharma PK, Banik A. recent advances on microsponge delivery system. *Int J Pharm Sci Res*. 2011;8(2):13-23.

30. Jadhav N, Patel V, Mungekar S, Bhamare G, Karpe M. Microsponge Delivery System : An updated review , current status and future prospects. *J Sci Innov Res*. 2013;2(6):1097-1110.

31. Parikh BN, Gothi GD, Patel TD, Chavda H V., Patel CN. Microsponge as novel topical drug delivery system. *J Glob Pharma Technol*. 2010;2(1):17-29. doi:10.1016/S0969-6997(11)00073-1

32. Abdelmalak NS, El-Menshawe SF. A new topical fluconazole microsponge loaded hydrogel: preparation and characterization. *Int J Pharm Pharm Sci*. 2012;4(1):460-468.

33. Srivastava R, Puri V, Srimal RC, Dhawan BN. Effect of curcumin on platelet aggregation and vascular prostacyclin synthesis. *Arzneimittelforschung*. 1986;36(4):715-717. http://www.ncbi.nlm.nih.gov/pubmed/3521617.

34. Arya P, Pathak K. Assessing the viability of microsponges as gastro retentive drug delivery system of curcumin: Optimization and pharmacokinetics. *Int J Pharm*. 2014;460(1-2):1-12. doi:10.1016/j.ijpharm.2013.10.045

35. Junqueira M V, Borghi-pangoni FB, Bruschi ML. Methodology for Methylene Blue Analysis from Polymeric Systems Used in Photodynamic Therapy : Comparison of Two Methods for Quantification. *Lat Am J Pharm*. 2018;37(1):105-112.

619 36. Pandey P, Jain V, Mahajan S. A review: microsponge drug delivery system. *Int J*
620 *Biopharm*. 2013;4(3):225-230. doi:10.1056/NEJM197302222880814
621 37. Villa Nova M, Gonçalves M de CP, Nogueira AC, et al. Formulation and
622 characterization of ethylcellulose microparticles containing L-alanyl-L-glutamine
623 peptide. *Drug Dev Ind Pharm*. 2013;9045:1-10. doi:10.3109/03639045.2013.817417
624 38. Korsmeyer RW, Gurny R, Doelker E, Buri P, Peppas NA. Mechanisms of solute
625 release from porous hydrophilic polymers. *Int J Pharm*. 1983;15:25-35.
626 doi:10.1016/0378-5173(83)90064-9
627 39. Folzer E, Gonzalez D, Singh R, Derendorf H. Comparison of skin permeability for
628 three diclofenac topical formulations: An in vitro study. *Pharmazie*. 2014;69(Table
629 2):27-31. doi:10.1691/ph.2014.3087
630 40. Pierre MBR, Lopez RF V, Bentley MVLB. Influence of ceramide 2 on in vitro skin
631 permeation and retention of 5-ALA and its ester derivatives, for Photodynamic
632 Therapy. *Brazilian J Pharm Sci*. 2009;45:109-116. doi:10.1590/S1984-
633 82502009000100013
634 41. Junqueira M V., Borghi-Pangoni FB, Ferreira SBS, Rabello BR, Hioka N, Bruschi ML.
635 Functional Polymeric Systems as Delivery Vehicles for Methylene Blue in
636 Photodynamic Therapy. *Langmuir*. 2016;32(1):19-27.
637 doi:10.1021/acs.langmuir.5b02039
638 42. Baesso ML, Shen J, Snook RD. Laser-induced photoacoustic signal phase study of
639 stratum corneum and epidermis. *Analyst*. 1994;119(4):561-562.
640 doi:10.1039/an9941900561
641 43. Borghi-Pangoni FB, Junqueira MV, de Souza Ferreira SB, et al. Preparation and
642 characterization of bioadhesive system containing hypericin for local photodynamic
643 therapy. *Photodiagnosis Photodyn Ther*. 2017;19(June):284-297.

644 doi:10.1016/j.pdpdt.2017.06.016
645 44. Ames FQ, Sato F, de Castro L V., et al. Evidence of anti-inflammatory effect and
646 percutaneous penetration of a topically applied fish oil preparation: a photoacoustic
647 spectroscopy study. *J Biomed Opt*. 2017;22(5):055003.
648 doi:10.1117/1.JBO.22.5.055003
649 45. Kumari A, Jain A, Hurkat P, Verma A, Jain SK. Microsponges : A Pioneering Tool for
650 Biomedical Applications. *Ther drug Carr Syst*. 2016;33(1):77-105.
651 46. Rowe RC, Sheskey PJ, Quinn ME. *Handbook Pharmaceutical Excipients*. 6th ed.
652 Pharmaceutical Press; 2009.
653 47. Junqueira MV, Bruschi ML. A Review About the Drug Delivery from Microsponges.
654 *AAPS PharmSciTech*. 2018;19(4):1501-1511. doi:10.1208/s12249-018-0976-5
655 48. Kwon J, Kim J, Park D, Han H. A novel synthesis method for an open-cell
656 microsponge polyimide for heat insulation. *Polymer (Guildf)*. 2015;56:68-72.
657 doi:10.1016/j.polymer.2014.06.090
658 49. Moghimipour E, Kargar M, Ramezani Z, Handali S. The potent in vitro skin permeation
659 of archeosome made from lipids extracted of *Sulfolobus acidocaldarius*. *Archaea.*
660 2013;Article ID 782012:1-7. doi: 10.1155/2013/782012
661 50. Davidovich-Pinhas M, Barbut S, Marangoni AG. Physical structure and thermal
662 behavior of ethylcellulose. *Cellulose*. 2014;21(5):3243-3255. doi:10.1007/s10570-014-
663 0377-1
664 51. Albadarin AB, Potter CB, Davis MT, et al. Development of stability-enhanced ternary
665 solid dispersions via combinations of HPMCP and Soluplus®processed by hot melt
666 extrusion. *Int J Pharm*. 2017;532(1):603-611. doi:10.1016/j.ijpharm.2017.09.035
667 52. Chorilli M, Brizante AC, Rodrigues CA, Salgado HRN. Aspectos gerais em sistemas
668 transdérmicos de liberação de fármacos. *Rev Bras Farm*. 2007;88(1):7-13.

669 53. Sohi H, Ahuja A, Ahmad FJ, Khar RK. Critical evaluation of permeation enhancers for
670 oral mucosal drug delivery. *Drug Dev Ind Pharm*. 2010;36(3):254-282.
671 doi:10.3109/03639040903117348
672 54. Azevedo RB, Faber J, Leal S, Lucci C. Histologia Da Cavidade Oral. In: *Sistema*
673 *Digestório: Integração Básico-Clínica*. ; 2016. http://pdf.blucher.com.br.s3-sa-east-
674 1.amazonaws.com/openaccess/9788580391893/09.pdf.
675 55. Lundblad RL. *Biochemistry and Molecular Biology Compendium*. 1st Edition.; 2007.
676 doi:10.1201/9781420043488
677 56. Lundblad RL, Macdonald F. *Handbook of Biochemistry and Molecular Biology*. Fifth
678 Edit. CRC Press; 2018. doi:10.1201/b21846
679 57. Oliveira De Melo J, Pedrochi F, Baesso ML, et al. Evidence of deep percutaneous
680 penetration associated with anti-inflammatory activity of topically applied Helicteres
681 gardneriana extract: A photoacoustic spectroscopy study. *Pharm Res*. 2011;28(2):331-
682 336. doi:10.1007/s11095-010-0279-3
683 58. Mota JP, Carvalho JLC, Carvalho SS, Barja PR. Photoacoustic techique applied to skin
684 research: characterization of tissue, topically applied products and transdermal drug
685 delivery. In: Beghi PMG, ed. *Acoustic Waves: From Microdevices to Helioseismology*.
686 Rijka; 2011:652.
687